

Received May 27, 2020, accepted June 8, 2020, date of publication June 11, 2020, date of current version June 23, 2020.

Digital Object Identifier 10.1109/ACCESS.2020.3001580

A High Sensitivity 20-MHz Endoscopic Transducer With Integrated Miniature Amplifier

ZHILE HAN^{1,2}, (Member, IEEE), JIE XU^{1,2}, CHEN YANG², NINGHAO WANG²,
ZHANGJIAN LI², (Member, IEEE), YAOLAO CUI², (Member, IEEE),
AND XIAOHUA JIAN², (Member, IEEE)

¹Academy for Engineering and Technology, Fudan University, Shanghai 200433, China

²Suzhou Institute of Biomedical Engineering and Technology, Chinese Academy of Sciences, Suzhou 215163, China

Corresponding author: Xiaohua Jian (jianxh@sibet.ac.cn)

This work was supported in part by the National Key Research and Development Program of China under Grant 2019YFC0120500 and Grant 2018YFC0116201, in part by the National Natural Science Foundation of China under Grant 21927803 and Grant 11704397, and in part by the Funds of Youth Innovation Promotion Association, Chinese Academy of Sciences, under Grant Y201961 and Grant YJKYYQ20180031.

ABSTRACT Endoscopic transducer with small size and high frequency has been widely studied and applied in medical ultrasound imaging. However, attenuation affects high frequency ultrasound waves to a greater degree than lower frequency waves, which results in limited endoscopic ultrasound detection depth and poor signal-to-noise ratio in the image. High sensitivity transducer is an effective way to improve this problem. In this paper, a high sensitivity endoscopic ultrasound transducer (HSEUST) with an integrated miniature amplifier was proposed, where the amplifier can effectively enhance the received ultrasound signal and reduce the impact of noise. According to the tests and experimental results, this sensor is about 4 times more in sensitive, 20% more in resolution than conventional endoscopic transducer. With high sensitivity, this transducer holds the potential for visualization of deeper tissue in the body with high resolution, which will greatly expand the application capabilities and fields of endoscope ultrasound imaging.

INDEX TERMS Endoscopic transducer, high frequency, high sensitivity.

I. INTRODUCTION

High frequency endoscopic ultrasound transducer is widely used in many medical applications like digestive and lung disease assessment [1], transoesophageal ultrasound-guided fine-needle aspiration (EUS-FNA) [2], transbronchial ultrasound-guided needle aspiration (EBUS-TBNA) [3] and so on. In comparison with conventional in vitro transducer, endoscopic transducer usually has a higher frequency, smaller size, and longer connection cables [4], [5]. For example, the current clinical use of digestive ultrasound endoscopic transducer is operating at 12 / 20 MHz, 1.5 mm in diameter and 2.4 m in cable length.

For getting higher spatial resolution of ultrasound imaging to improve the accuracy of diagnosis, the higher frequency ultrasound was applied in EUS [6]. However, high-frequency ultrasound has to face the disadvantages of larger attenuation coefficient and shorter propagation path than low frequency ultrasound, which exponentially decayed with the frequency.

The associate editor coordinating the review of this manuscript and approving it for publication was Vishal Srivastava.

Furthermore, the long connection cable will greatly attenuate the received ultrasonic echo signal too [7], which will further limit the imaging depth and performance of EUS. However, if high-frequency ultrasound can combine imaging depth with high imaging resolution, this will be helpful for disease diagnosis and treatment like ultrasound-guided needle aspiration.

To achieve deeper imaging depth with high frequency, several possible options have been proposed. For example, increasing the transmitter power of the ultrasound transducer to increase the signal intensity, but simply turning up transmitting energy is not an option as a higher power ultrasound may damage the tissue [8]. Coded excitation can improve the signal-to-noise ratio (SNR) and penetration depth of high-frequency ultrasound imaging like intravascular ultrasound imaging (IVUS) [9], [10]. However, this method is limited by the capability of the transducer and system itself.

An alternative method would be to increase the sensitivity of an ultrasound transducer. Given the ultrasound radiation safety limit, the higher the detection sensitivity of the employed transducer the deeper the penetration capability of the ultrasound device. To achieve high sensitivity transducer,

many methods have been tried. For example, in the material, piezoelectric single crystals like PMN-PT, PIN-PMN-PT, and 1-3 piezoelectric composite materials have been developed [11]–[14]. In terms of the matching layer, multi-layers matching optimization is applied [15]. In the circuit, electrical resistance matching can also improve the signal intensity of the transducer [16]. In the frequency range, multifrequency or broadband ultrasound transducers were adopted to increase the detection signals [17], [18]. These methods all can improve the detector sensitivity to a certain extent, but the effect is still limited, for example, the single crystal PMN-PT composite with wide bandwidth can improve sensitivity by about 20~75% [19]–[21], the multiple matching layers can improve sensitivity by about 10%~50% [22], [23], the electrical resistance matching can improve sensitivity by about 10%~120% [24].

In addition to the above methods, integrating ultrasound transducer with front-end circuits is an efficient way to enhance the signal [25]–[27]. Array / Matrix transducer with custom application-specified integrated circuits (ASIC) has been previously demonstrated in ultrasound imaging [28]–[30]. For example, a 2D array transducer with integrated ASIC in a 10 Fr catheter was developed for real-time 3D intracardiac echocardiography [31]. Especially in the development of capacitive micromachined ultrasonic transducer (CMUT), because of its MEMS/CMOS-based process, the front-end circuits or ASIC is more and more adopted and integrated [32]–[36]. However, because the front-end circuits or ASIC chips are generally developed exclusively and mainly for multi-element ultrasound transducers, and they were not easy and suitable to be used with single-element transducer. Moreover, the production process of front-end and ASIC is complex, their research and development requirements and costs are high. In addition, especially for single element ultrasound transducer, it is hard to find a suitable front-end circuit or ASIC to integrate. Therefore, it will be valuable to find a method that can be combined with a conventional transducer to improve their detection sensitivity and imaging quality.

Therefore, based on recent progress on microelectronics technology and semiconductor processes, a high sensitivity endoscopic ultrasound transducer (HSEUST) with the integrated miniature amplifier is proposed in this paper, where the amplifier can provide an additional gain of the received ultrasound signal in 20 dB or more. Compared to the conventional post-gain amplifier method, this method can increase the original signal before the cable decays, thus effectively increasing the signal-to-noise ratio and imaging depth.

II. DESIGN AND FABRICATION OF HSEUST

At present, the amplifiers are usually rear-mounted in the ultrasonic endoscopy systems, the long transmission wire/cable will greatly reduce the echo signal and the final imaging quality. Since the maximum voltage limit of the micro amplifier is only 5V, while the excitation voltage of endoscopic transducer is 90 V for getting high enough

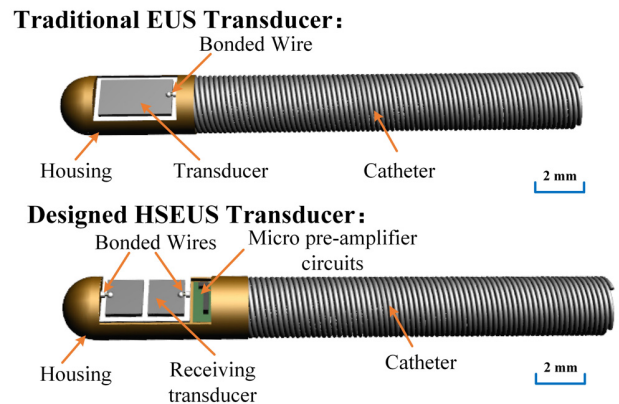


FIGURE 1. The designed diagram of the traditional EUS transducer and HSEUS transducer.

signal intensity. If the transmit and receive (TR) switch is used, the circuit structure will be more complex and larger. That's because TR switch means high-voltage process, and the micro amplifier is low-voltage work, if integrated TR into the front amplification circuit, the chip will require the high and low voltage process must be met at the same time, which will greatly increase the development of the process requirements and difficulty. Besides, the transducer and catheter size is strictly limited in endoscopic imaging. At present, the diameter of the mechanical rotary ultrasonic endoscope catheter is in the range of 1.4 to 2.6 mm, and the diameter of the transducer is in the range of 0.5 to 1.5 mm, respectively.

Therefore, We divided the transducer into two parts, both transmitter and receiver, in order to avoid device damage and maintain sufficient transmit power and echo signal strength. Specifically, in our design, a micro integrated front-end amplifier is integrated with the ultrasound receiver, which can efficiently process signals locally and maintain the signal integrity. In order to maintain the size of EUS transducer and the simplicity of the structure, the basic idea of our solution is to use the dual trans element mode. Therefore, a HSEUST was designed just as FIGURE. 1. showed.

The HSEUST consists of a transmitting transducer and a receiving transducer, which was connected with a micro amplifier board. These two transducers were in the same size of 1.45 mm × 1.50 mm × 0.8 mm, and their center frequency is 20 MHz. In order to prevent the high-voltage transmitting pulse (~90 V) to breakdown the amplification circuit, the two transducers are physically isolated, and the width of the kerf between them is 0.1 mm. While the contrasting transducer EUST, it uses the same material as HSEUST, except that its size is 3.0 mm × 1.50 mm × 0.8 mm, and it was directly bonded with the coaxial wire without the micro pre-amplifier. The circuit schematic of the designed HSEUST was as shown in Fig.2. It contains two parts transmitter and receiver with the micro amplifier.

Especially, the micro amplifier is a wideband high gain amplifier offering high dynamic range, which can work from 0.5 MHz to 100 MHz, and have a gain of more than 24 dB at 20 MHz. Its schematic was shown in Fig.3. It uses an

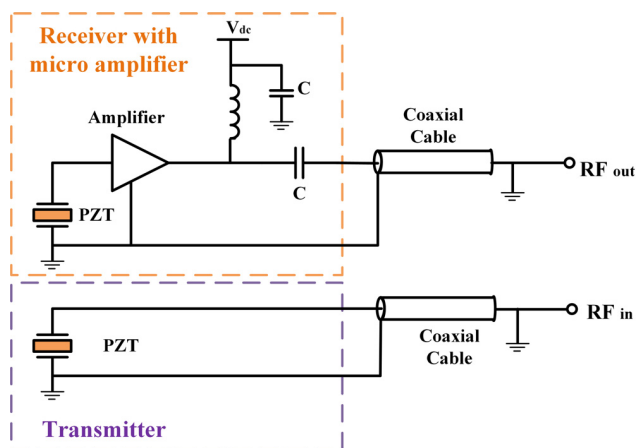


FIGURE 2. Circuit schematic of designed HSEUST.

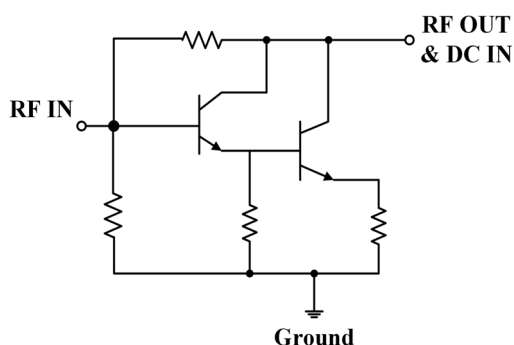


FIGURE 3. The schematic of micro amplifier.

improved Darlington configuration, which enables a large gain, high stability, and small size without increasing the connecting cable. It only needs a bias tee composed of a $1\mu\text{H}$ inductor L and a 10 nF capacitor C as DC bias to work. The value of the inductor L needs to be sufficiently high to prevent loss of echo signal due to the bias connection. A 10 nF capacitor C was properly chosen for DC blocking and AC coupling to RF out. The micro amplifier die has a $50\ \Omega$ output impedance to match with the connecting coaxial cable. The amplifier was fabricated using InGaP HBT technology. The amplifier die was in the size of $820 \times 760\ \mu\text{m}$ with 4 bond pads of $100 \times 100\ \mu\text{m}$, which enables tight integration with endoscopic transducers.

The measured output gain of the integrated amplifier circuits during $0\sim 100\text{ MHz}$ as shown in Fig.4. The measured -3 dB bandwidth ranges from 3.5 MHz to 56.4 MHz , making the amplifier suitable for detecting the endoscopic imaging signals. Notably, the amplifier shows a flat response of over 27 dB gain from 10 to 30 MHz , which can completely cover the bandwidth of the fabricated EUST transducer with the center frequency 20 MHz .

The measured output noise spectral density of the integrated amplifier circuits during $0\sim 50\text{ MHz}$ as shown in Fig.5. The noise density at 20 MHz was $15.42\text{ nV}/\sqrt{\text{Hz}}$ and the integrated noise level from 1 to 50 MHz was $161\ \mu\text{V}$. So the noise

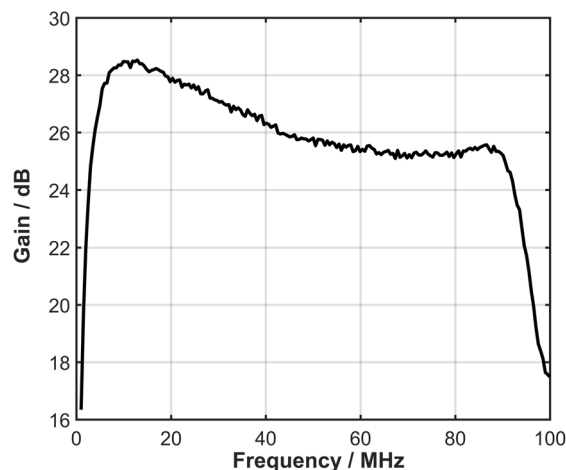


FIGURE 4. The measured gain of the micro amplifier during $0\sim 100\text{ MHz}$.

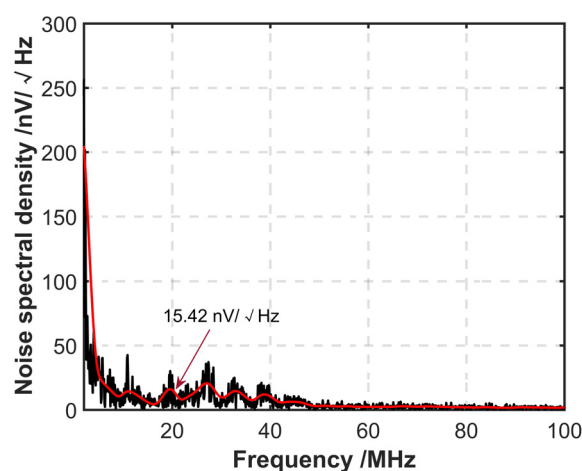


FIGURE 5. The measured output noise spectral density of the micro amplifier during $0\sim 100\text{ MHz}$.

of the amplifier is very small and will not affect the transducer echo waveform, which is usually at the mV magnitude.

During the fabrication process, firstly a 20 MHz PZT transducer of $3\text{ mm} \times 1.5\text{ mm}$ was made up of a $100\ \mu\text{m}$ PZT-5H as the active layer, a $650\ \mu\text{m}$ silver epoxy (E-solder 3022, Von Roll Isola Inc.) as the backing layer and a $35\ \mu\text{m}$ mixture matching layer. Then, the transducer was attached to the amplifier micro PCB board with silver epoxy (H20E, EpoTek). For the convenience of welding behind, the PZT layer gold electrode of the receiving transducer part was exposed at the edge. And then, the top electrode of the receiving transducer was interfaced to the input pad of the amplifier die by wire bonding, just as Fig.6 shows. All bonding gold wires in the diameter of $25\ \mu\text{m}$ were kept as short as possible to reduce performance degradation caused by series inductance.

After wire bonding and PCB surface ultraviolet glue protection, the transducer was diced into a transmitting transducer and a receiving transducer by a dicing saw (DAD3350, DISCO Corporation, Japan) with 0.1 mm soft diamond blade.

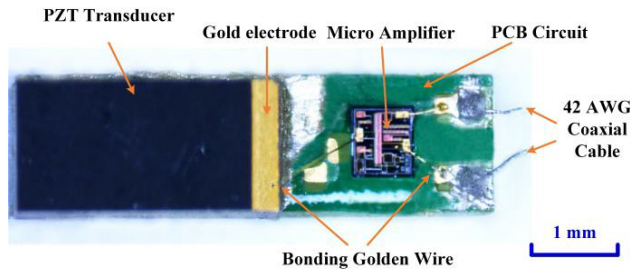


FIGURE 6. The fabricated transducer with integrated micro amplifier before dicing.

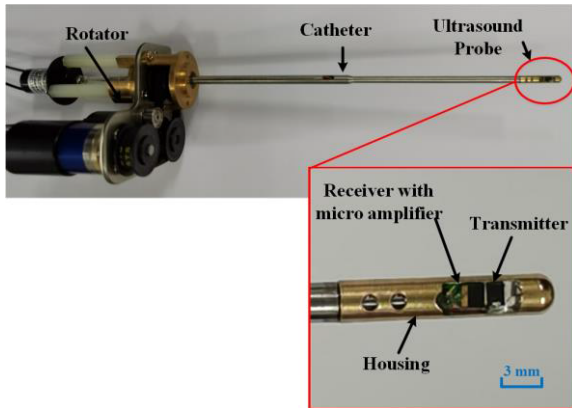


FIGURE 7. The image of fabricated HSEUST.

A 2.4-m long 42 AWG coaxial cables for RF output and DC power supply, was soldered to the corresponding pads on the receiving amplifier circuit. And another 2.4-m long coaxial wires was bonding to the upper and back surfaces of transmitting transducer with conductive silver epoxy. The whole HSEUST was fixed to the distal of a 2.5 mm diameter metal catheter with cc glue. The final fabricated HSEUST was as shown as Fig.7.

III. CHARACTERIZATION OF TRANSDUCER

To compare, a conventional 20 MHz endoscopic transducer (EUST) without micro pre-amplifier was produced. The contrasting transducer was made of the same material as HSEUST, in addition to its active layer using bulk PZT-5H ceramic, but it is 3 mm × 1.50 mm × 0.8 mm in size, which is same as the overall size of HSEUST. No pre-amplifier was connected to the EUST.

A DPR500 (pulse amplitude: 90 V, gain: 0 dB, filter: 5~300 MHz, RPF: 200 Hz, JSR Ultrasonics, USA) was used as the pulse-receiver to measure the center frequency, -6 dB bandwidth and pulse-echo amplitude of the fabricated HSEUST. The pulse-echo response was measured by recording the reflection from a quart polyethylene plastics flat placed at 5 mm in front of the transducer. The measured center frequency is 20.33 MHz for HSEUST and 20.97 MHz for EUST, respectively. They are almost the same in center frequency. As shown in Fig.9, the -6 dB bandwidth is 47.03% for HSEUST and 42.19% for EUST, respectively. Therefore, the design of HSEUST does not affect the bandwidth of

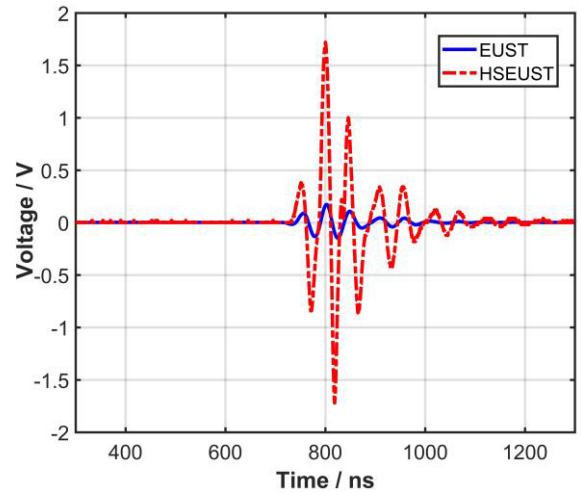


FIGURE 8. The pulse-echo waveforms of fabricated HSEUST and contrasting EUST.

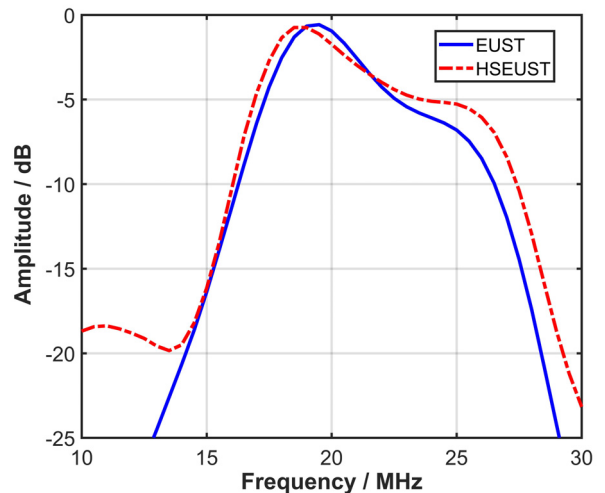


FIGURE 9. The pulse-echo frequency spectrums of fabricated HSEUST and contrasting EUST.

transducer, but has some improvements. And in terms of the pulse half-width, it is 77.6 ns for HSEUST while 99.2 ns for EUST, just as Fig.8 and Fig.9 show. Because the ultrasound imaging resolution is directly related to the pulse width, the HSEUST can effectively improve the resolution by more than 20%. Especially, for the echo intensity, the HSEUST amplitude was measured as 3.44 V with 50 Ω coupling impedance setting, while it is only 0.7 V for EUST. As a result, the HSEUST increased the detection signal by about five times.

To find out how much contribution came from the HSEUST structure and how much from the amplifier, another set of comparative experiments with the same structure of HSEUST, just one with the amplifier, the other did not. The test echo results are shown in Fig.10. From the figure it can be found that without the amplifier, the peak-to-peak of HSEUST is only 0.51 V, while the HSEUST with amplifier has 3.44 V, which is almost 7 times the HSEUST

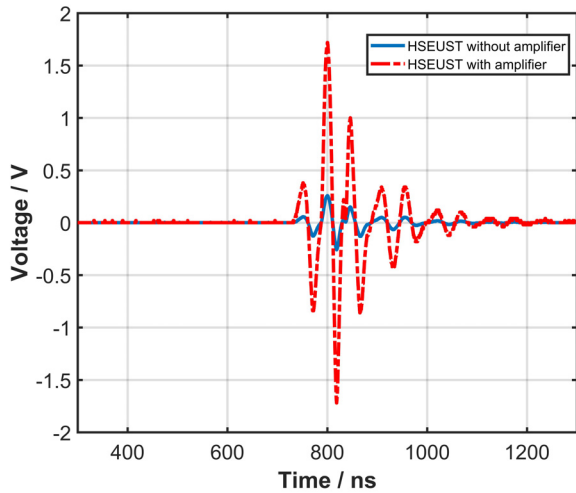


FIGURE 10. The pulse-echo waveforms of HSEUST(with amplifier) and contrasting HSEUST(without amplifier).

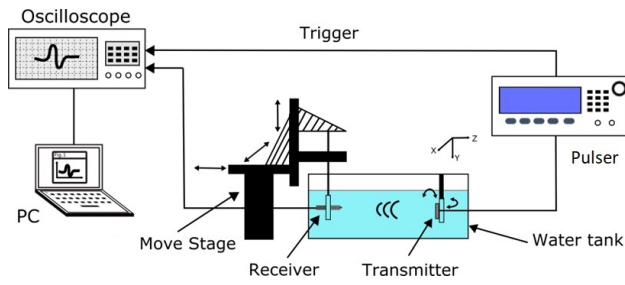


FIGURE 11. The transducer transmitting testing system.

without amplifier. In addition, HSEUST without an amplifier has a lower peak-to-peak than the traditional EUST of the same volume, which is 0.7 V. Furthermore, the noise of amplifier is very small and does not affect the waveform and spectrum. Therefore, it can be considered that most of these improvements were due to the integration of the micro amplifier.

The insertion loss IL is the loss of signal power resulting from the insertion of a device in a transmission line, which is defined as the ratio (in dB) of the output power of the transducer to the input power delivered by the electrical source, just as shown in Eq.(1). In our case, the insertion loss of HSEUST and EUST was -26.19 dB and -39.97 dB, respectively. This means that HSEUST can decrease the insertion loss by 13.78 dB.

$$IL = 10 \lg\left(\frac{P_{out}}{P_{in}}\right) = 20 \lg\left(\frac{V_{out}\sqrt{R_{in}}}{V_{in}\sqrt{R_{out}}}\right) \quad (1)$$

The signal-to-noise ratio (SNR) compares the level of the desired signal to the level of background noise. SNR is defined as the ratio of signal power to the noise power, often expressed in decibels. According to Eq.(2), the SNR of HSEUST and EUST was 11.39 dB and 23.99 dB, respectively. This means that HSEUST can increase SNR by 12.60 dB, which will be helpful to improve imaging quality.

$$SNR = 10 \lg\left(\frac{P_{signal}}{P_{noise}}\right) = 20 \lg\left(\frac{V_{signal}^2}{V_{noise}^2}\right) \quad (2)$$

TABLE 1. Summary of performance characterization.

	EUST	HSEUST
Center Frequency	20.97 MHz	20.33 MHz
Bandwidth @-6 dB	42.19%	47.03%
Echo Peak	0.70 V	3.44 V
Pulse width@-6 dB	99.2 ns	77.6 ns
Pulse width@-6 dB	-39.97 ns	-26.19 ns
Receiving sensitivity	7.8 mV/V	38.2 mV/V
Transmitting sensitivity	17.89 KPa/V	17.03 Kpa/V

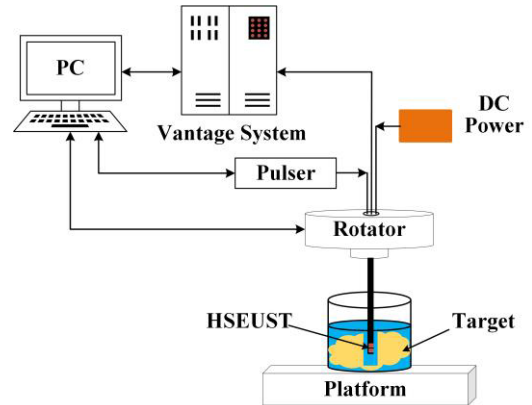


FIGURE 12. The schematic of the imaging experimental system.

Further, the receiving sensitivity of HSEUST and EUST, which is defined as the ratio of the peak amplitude of the echo signal to the excitation pulse, was evaluated. They are 38.2 mV/V and 7.8 mV/V, respectively. So the HSEUST receiving sensitivity is about 5 times than EUST.

To characterize the transmitting sensitivity of the fabricated HSEUST, a testing system was set up just as Fig.11 showed. In transmitting sensitivity testing, a PVDF needle hydrophone with a diameter of 0.2 mm (Precision Acoustics, UK) was used as the detector. The tested transducer was placed 5 mm away from the hydrophone. The measured transducer was driven by a negative voltage pulse of 5 ns pulse width, 200 Hz repeat frequency, and 90 V peak amplitude generated by a DPR 500. The detected signals of hydrophone were averaged 16 times and recorded by an oscilloscope (DPO5034, Tektronix) for offline analysis. The final detected amplitude of HSEUST and EUST was 93.47 mV and 98.19 mV, respectively. According to the sensitivity of hydrophone at 20 MHz is 61 nV/Pa, the final transmitting sensitivity of HSEUST and EUST was 17.03 Kpa/V and 17.89 KPa/V, respectively. Thus, although the working area of HSEUST is about half smaller of EUST, the transmitting sensitivity of the two is not much different.

The measured performance characterizations of HSEUST and EUST was listed in Tab.1.

IV. EXPERIMENTAL RESULTS AND DISCUSSIONS

Images of an in-vitro phantom (stomachs of swine) were acquired to validate the performance of the HSEUST developed in this work. Fig.12 illustrates the overall architecture of the imaging experiment system. In the transmitting part,

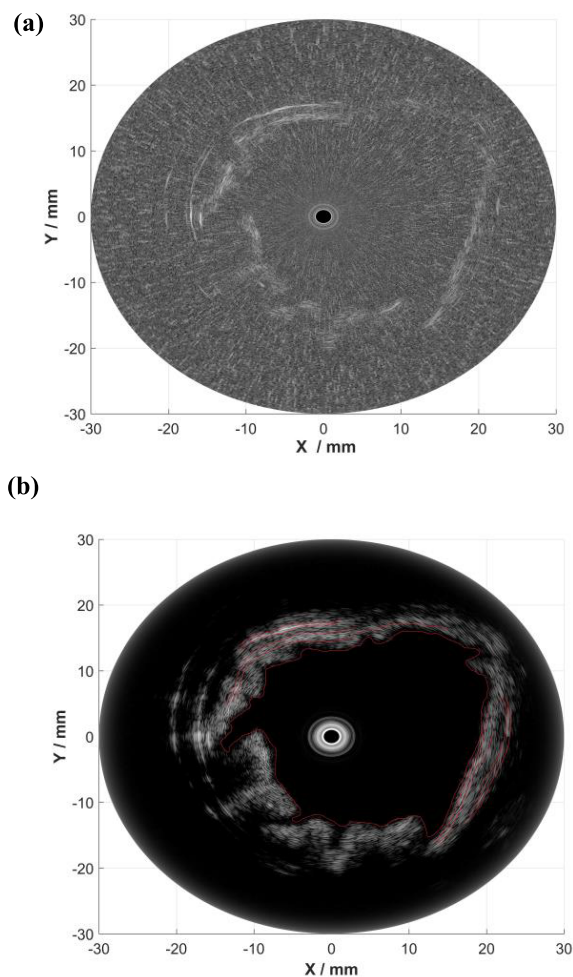


FIGURE 13. The images of swine stomach phantom detected by: (a) EUST; (b) HSEUST.

a pulser (DPR500, pulse amplitude: 90 V, RPF: 200 Hz, Energy per pulse: $2.5 \mu\text{J}$, JSR Ultrasonics, USA) was used to stimulate the transmitting transducer. In the receiving part, a DC power (5V, E3631A, Keysight Technologies, USA) supply the working power of the micro-amplifier-circle, the Vantage System (Vantage 64 LE HF Verasonics, America) was used as the ultrasound system platform on which we can program ultrasound information including signal receiving and processing.

To form an A-line, the acoustic waves emitted from the transmitter part of HSEUST were detected by the receiving part of HSEUST, placed at the tip of the catheter. Then, the echo electrical signals were firstly amplified by the micro amplifier of HSEUST, then transmitted and attenuated by the 2.4-m long cable, and entered the Vantage System. The signal was amplified using a low noise amplifier (LNA, Gain 12 dB, High-pass frequency 50 kHz) and digitized via an 80 MSPS data acquisition (DAQ) card in the Vantage system, and finally stored into a personal computer (PC). Cross-sectional image (B-scan) data were recorded by rotating the catheter with respect to its central axis via a precious DC-micromotors

(RE22, Maxon Motor AG, Switzerland), which can reach 1200 rounds per minute under PC control. A photoelectric encoder (E6A2, OMRON Corporation, Japan) is used to record the location of each A-line data and to reconstruct the image. Specifically, the photoelectric encoder gives the pulse generator a trigger signal to generate an excitation pulse for the transducer, and control the motor in the process of rotating a circle to produce 512 sets of echo data for the construction of an image. The acquired signals were band-pass filtered (bandwidth: 5–50 MHz), followed by Hilbert transform, and then converted to the polar coordinates for display (signal processing performed with MATLAB).

The obtained phantom images were shown in Fig.13. A dynamic range of 60 dB was used for both images, and the depth of the image display is 30 mm, which is more than twice the imaging depth of the current commercial 20 MHz ultrasound endoscope system. As shown in Fig.10, it is obvious that the image acquired by the HSEUST looks much clear and sharper than that captured by the conventional EUST transducer. The 5 layers of swine stomach wall can be clearly visualized from the image detected by HSEUST, while only 2 layer boundary was showed in the image detected by EUST. Specifically, the imaging resolution of the EUST transducer was found to be $151 \mu\text{m}$, while for the HSEUST they were $122 \mu\text{m}$, respectively. The penetration depth of the EUST is about 15 mm, while although limited by the size of the phantom, the penetration depth of fabricated HSEUST was around 30 mm, which can be deeper and would be sufficient for diagnosis.

V. CONCLUSION

A high sensitivity endoscopic ultrasound transducer with an integrated miniature amplifier was studied in this paper, where the amplifier can effectively enhance the received ultrasound signal. A prototype of HSEUST with a center frequency of 20 MHz was designed and fabricated. According to the tests and experimental imaging results, HSEUST is about 4 times more in sensitive, 20% more in resolution than conventional endoscopic transducer. With high sensitivity, HSEUST holds the potential for visualization of deeper tissue in the body with high resolution, which will greatly expand the application capabilities and fields of endoscope ultrasound imaging. And the signal to noise ratio and image quality of the image has also been significantly improved by HSEUST, which will be very useful for the weak signal processing of high frequency ultrasound imaging.

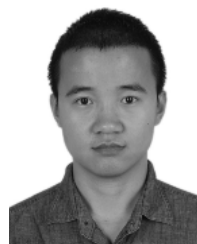
ACKNOWLEDGMENT

(Zhile Han and Jie Xu contributed equally to this work.)

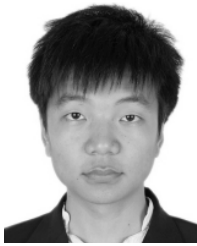
REFERENCES

- [1] F. J. F. Herth, R. Eberhardt, M. Krasnik, and A. Ernst, "Endobronchial ultrasound-guided transbronchial needle aspiration of lymph nodes in the radiologically and positron emission tomography-normal mediastinum in patients with lung cancer," *Chest*, vol. 133, no. 4, pp. 887–891, Apr. 2008.
- [2] R. A. Erickson, L. Sayagerabie, and A. Avotsavotins, "Clinical utility of endoscopic ultrasound-guided fine needle aspiration," *Acta Cytologica*, vol. 41, no. 6, p. 1647, 1997.

- [3] T. Nakajima, K. Yasufuku, M. Suzuki, K. Hiroshima, R. Kubo, S. Mohammed, Y. Miyagi, S. Matsukuma, Y. Sekine, and T. Fujisawa, "Assessment of epidermal growth factor receptor mutation by endobronchial ultrasound-guided transbronchial needle aspiration," *Chest*, vol. 132, no. 2, pp. 597–602, Aug. 2007.
- [4] H. Adachi, K. Wakabayashi, A. Mizunuma, Y. Sawada, T. Imahashi, T. Fujimura, and D. O. H. Ki, "Ultrasound transducer manufactured by using micromachining process, its device, endoscopic ultrasound diagnosis," U.S. Patent 7 982 362 B2, Jul. 19, 2011.
- [5] F. E. Silverstein, R. W. Martin, M. B. Kimmey, G. C. Jiranek, D. W. Franklin, and A. Proctor, "Experimental evaluation of an endoscopic ultrasound probe: *In vitro* and *in vivo* canine studies," *Gastroenterology*, vol. 96, no. 4, pp. 1058–1062, Apr. 1989.
- [6] D. P. Hurlstone, S. S. Cross, and D. S. Sanders, "20-MHz high-frequency endoscopic ultrasound-assisted endoscopic mucosal resection for colorectal submucosal lesions: A prospective analysis," *J. Clin. Gastroenterol.*, vol. 39, no. 7, pp. 596–599, 2005.
- [7] X. Jian, Z. Li, Z. Han, J. Xu, P. Liu, Y. Liu, Y. Cui, and W. Huang, "The study of cable effect on high-frequency ultrasound transducer performance," *IEEE Sensors J.*, vol. 18, no. 13, pp. 5265–5271, Jul. 2018.
- [8] P. R. Hoskins, K. Martin, and A. Thrush, *Diagnostic Ultrasound (Physics and Equipment) || Safety of Diagnostic Ultrasound*. Cambridge, U.K.: Cambridge Univ. Press, 2010, pp. 155–170, doi: 10.1017/CBO9780511750885.
- [9] W. Qiu, X. Wang, Y. Chen, Q. Fu, M. Su, L. Zhang, J. Xia, J. Dai, Y. Zhang, and H. Zheng, "Modulated excitation imaging system for intravascular ultrasound," *IEEE Trans. Biomed. Eng.*, vol. 64, no. 8, pp. 1935–1942, Aug. 2017.
- [10] R. Y. Chiao and X. Hao, "Coded excitation for diagnostic ultrasound: A system developer's perspective," *IEEE Trans. Ultrason., Ferroelectr., Freq. Control*, vol. 52, no. 2, pp. 160–170, Feb. 2005.
- [11] X. Jiang, K. Snook, A. Cheng, W. S. Hackenberger, and X. Geng, "Micro-machined PMN-PT single crystal composite transducers—15–75 MHz PC-MUT," in *Proc. IEEE Ultrason. Symp.*, Nov. 2008, pp. 164–167.
- [12] Z.-W. Yin, H.-S. Luo, P.-C. Wang, and G.-S. Xu, "Growth, characterization and properties of relaxor ferroelectric PMN-PT single crystals," *Ferroelectrics*, vol. 229, no. 1, pp. 207–216, May 1999.
- [13] S. Zhang, J. Luo, W. Hackenberger, N. P. Sherlock, and T. R. Shrout, "Electromechanical characterization of $\text{Pb}(\text{In}_{0.5}\text{Nb}_{0.5})\text{O}_3\text{-Pb}(\text{Mg}_{1/3}\text{Nb}_{2/3})\text{O}_3\text{-PbTiO}_3$ crystals as a function of crystallographic orientation and temperature," *J. Appl. Phys.*, vol. 105, no. 10, May 2009, Art. no. 104506.
- [14] F. Li, D. Lin, Z. Chen, Z. Cheng, J. Wang, C. Li, Z. Xu, Q. Huang, X. Liao, L.-Q. Chen, T. R. Shrout, and S. Zhang, "Ultrahigh piezoelectricity in ferroelectric ceramics by design," *Nature Mater.*, vol. 17, pp. 349–354, Mar. 2018.
- [15] H. W. Persson and C. H. Hertz, "Acoustic impedance matching of medical ultrasound transducers," *Ultrasonics*, vol. 23, no. 2, pp. 83–89, Mar. 1985.
- [16] H. Huang and D. Paramo, "Broadband electrical impedance matching for piezoelectric ultrasound transducers," *IEEE Trans. Ultrason., Ferroelectr., Freq. Control*, vol. 58, no. 12, pp. 2699–2707, Dec. 2011.
- [17] C. Sun, Q. Shi, M. S. Yazici, T. Kobayashi, Y. Liu, and C. Lee, "Investigation of broadband characteristics of multi-frequency piezoelectric micro-machined ultrasonic transducer (MF-pMUT)," *IEEE Sensors J.*, vol. 19, no. 3, pp. 860–867, Feb. 2019.
- [18] C. Sun, S. Jiang, and Y. Liu, "Numerical study and optimisation of a novel single-element dual-frequency ultrasound transducer," *Sensors*, vol. 18, no. 3, p. 703, Feb. 2018.
- [19] D. Robertson, G. Hayward, A. Gachagan, and V. Murray, "Comparison of the performance of PMN-PT single-crystal and ceramic composite arrays for NDE applications," *Or Insight*, vol. 48, no. 2, pp. 97–100, 2006.
- [20] J. Yuan, S. Rhee, and X. N. Jiang, "60 MHz PMN-PT based 1-3 composite transducer for IVUS imaging," in *Proc. IEEE Ultrason. Symp.*, Nov. 2008, pp. 682–685.
- [21] X. Jian, S. Li, W. Huang, Y. Cui, and X. Jiang, "Electromechanical response of micromachined 1-3 piezoelectric composites: Effect of etched piezo-pillar slope," *J. Intell. Mater. Syst. Struct.*, vol. 26, no. 15, 2014, Art. no. 1045389X14546657.
- [22] A. J. Mulholland, N. Ramadas, R. L. O'Leary, A. C. S. Parr, G. Hayward, A. Troge, and R. A. Pethrick, "Enhancing the performance of piezoelectric ultrasound transducers by the use of multiple matching layers," *IMA J. Appl. Math.*, vol. 73, no. 6, pp. 936–949, Nov. 2008.
- [23] T. Inoue, M. Ohta, and S. Takahashi, "Design of ultrasonic transducers with multiple acoustic matching layers for medical application," *IEEE Trans. Ultrason., Ferroelectr., Freq. Control*, vol. 34, no. 1, pp. 8–16, Jan. 1987.
- [24] V. T. Rathod, "A review of electric impedance matching techniques for piezoelectric sensors, actuators and transducers," *Electronics*, vol. 8, no. 2, p. 169, Feb. 2019.
- [25] H. Choi, X. Li, S.-T. Lau, C. Hu, Q. Zhou, and K. K. Shung, "Development of integrated preamplifier for high-frequency ultrasonic transducers and low-power handheld receiver," *IEEE Trans. Ultrason., Ferroelectr., Freq. Control*, vol. 58, no. 12, pp. 2646–2658, Dec. 2011.
- [26] H. Choi, X. Li, S.-T. Lau, C. Hu, Q. Zhou, and K. K. Shung, "Development of integrated preamplifier for high frequency ultrasonic transducer," in *Proc. IEEE Int. Ultrason. Symp.*, Oct. 2010, pp. 1964–1967.
- [27] H. S. Lay, M. P. Y. Desmulliez, S. Cochran, G. Cummins, B. F. Cox, Y. Qiu, M. V. Turcanu, R. McPhillips, C. Connor, R. Gregson, and E. Clutton, "In-vivo evaluation of micro-ultrasound and thermometric capsule endoscopes," *IEEE Trans. Biomed. Eng.*, vol. 66, no. 3, pp. 632–639, Mar. 2019.
- [28] G. Gurun, P. Hasler, and F. L. Degertekin, "A 1.5-mm diameter single-chip CMOS front-end system with transmit-receive capability for CMUT-on-CMOS forward-looking IVUS," in *Proc. IEEE Int. Ultrason. Symp.*, Oct. 2011, pp. 478–481.
- [29] C. Chen, E. Noothout, H. J. Vos, J. G. Bosch, M. D. Verweij, N. de Jong, M. A. P. Pertijs, S. B. Raghunathan, Z. Yu, M. Shabanmottlagh, Z. Chen, Z.-Y. Chang, S. Blaak, C. Prins, and J. Ponte, "A prototype PZT matrix transducer with low-power integrated receive ASIC for 3-D transesophageal echocardiography," *IEEE Trans. Ultrason., Ferroelectr., Freq. Control*, vol. 63, no. 1, pp. 47–59, Jan. 2016.
- [30] M. Tan, E. Kang, J.-S. An, Z.-Y. Chang, P. Vince, N. Senegond, and M. A. P. Pertijs, "An integrated programmable high-voltage bipolar pulser with embedded Transmit/Receive switch for miniature ultrasound probes," *IEEE Solid-State Circuits Lett.*, vol. 2, no. 9, pp. 79–82, Sep. 2019.
- [31] D. Wildes, W. Lee, B. Haider, S. Cogan, K. Sundaresan, D. M. Mills, C. Yetter, P. H. Hart, C. R. Haun, M. Concepcion, J. Kirkhorn, and M. Bitoun, "4-DICE: A 2-D array transducer with integrated ASIC in a 10-F catheter for real-time 3-D intracardiac echocardiography," *IEEE Trans. Ultrason., Ferroelectr., Freq. Control*, vol. 63, no. 12, pp. 2159–2173, Dec. 2016.
- [32] J. Lim, C. Tekes, F. L. Degertekin, and M. Ghovanloo, "Towards a reduced-wire interface for CMUT-based intravascular ultrasound imaging systems," *IEEE Trans. Biomed. Circuits Syst.*, vol. 11, no. 2, pp. 400–410, Apr. 2017.
- [33] H.-S. Yoon, C. Chang, J. H. Jang, A. Bhuyan, and B. Khuri-Yakub, "Ex vivo HIFU experiments using a 32×32 -element CMUT array," *IEEE Trans. Ultrason., Ferroelectr., Freq. Control*, vol. 63, no. 12, pp. 2150–2158, Dec. 2016.
- [34] S. Kothapalli, T.-J. Ma, S. Vaithilingam, O. Oralkan, B. T. Khuri-Yakub, and S. S. Gambhir, "Deep tissue photoacoustic imaging using a miniaturized 2-D capacitive micromachined ultrasonic transducer array," *IEEE Trans. Biomed. Eng.*, vol. 59, no. 5, pp. 1199–1204, May 2012.
- [35] I. Cicek, A. Bozkurt, and M. Karaman, "Design of a front-end integrated circuit for 3D acoustic imaging using 2D CMUT arrays," *IEEE Trans. Ultrason., Ferroelectr., Freq. Control*, vol. 52, no. 12, pp. 2235–2241, Dec. 2005.
- [36] A. Moini, A. Nikoozadeh, J. W. Choe, C. Chang, D. N. Stephens, D. J. Sahn, and P. T. Khuri-Yakub, "Fully integrated 2D CMUT ring arrays for endoscopic ultrasound," in *Proc. IEEE Int. Ultrason. Symp. (IUS)*, Sep. 2016, pp. 1–4.



ZHILE HAN (Member, IEEE) received the B.S. degree in mechatronics engineering from the Harbin Institute of Technology of China, Harbin, China, in 2011, and the Ph.D. degree from Fudan University, in September 2018. He is currently a Research and Development Engineer with Medical Ultrasound Department, Suzhou Institute of Biomedical Engineering and Technology, Chinese Academy of Sciences. He has authored and coauthored about ten journal articles and more than ten patents. His research interests include the study of high frequency intravascular ultrasound systems, especially for the structure design of interventional catheter and micro-transducer production process.



JIE XU received B.S. degree in mechanical and electrical engineering from the University of Chinese Academy of Sciences, China, in 2014, and the Ph.D. degree from Fudan University, in September 2018. He is currently an Assistant Researcher with the Medical Ultrasound Department, Suzhou Institute of Biomedical Engineering and Technology, Suzhou, China. His research interests include ultrasonic systems, ultrasound thrombolysis, and electronic circuit analysis and design.



ZHANGJIAN LI (Member, IEEE) received the B.S. degree in instrument science and technology from the University of Science and Technology of China, Hefei, China, in 2011, and the master's degree in optical engineering from the University of Chinese Academy of Sciences, Beijing, China, in 2014. He is currently a Research Assistant Fellow with the Suzhou Institute of Biomedical Engineering and Technology, Chinese Academy of Sciences, Suzhou, Jiangsu, China. He is currently with Medical Ultrasound Department. His research interest includes micro medical ultrasound transducer and its applications.



CHEN YANG received the B.S. degree in biomedical engineering from Xi'an Jiaotong-Liverpool University, Suzhou, China, in 2015. He is currently pursuing the Ph.D. degree with the University of Science and Technology of China, in 2017. He is currently working at the Suzhou Institute of Biomedical Engineering and Technology, Chinese Academy of Sciences, under the supervision of Dr. Yaoyao Cui. His research interest includes high frequency ultrasound transducer.



YAoyao CUI (Member, IEEE) received the Ph.D. degree in biomedical engineering from Xi'an Jiaotong University in 2002. She worked as a Postdoctoral Researcher and a Research Fellow from 2003 to 2010, with CREATIS, INSA de Lyon, the Medical Vision Laboratory, University of Oxford, and the Department of Physics Engineering, University of Dundee. She joined the Suzhou Institute of Biomedical Engineering and Technology (SIBET) in 2011 and set up a Medical Ultrasound Laboratory, which mainly focuses on the high-frequency ultrasound imaging, smaller size transducers, and their clinical applications, e.g., intravascular ultrasound, ultrasound endoscope, interventional ultrasound, and so on. She is a Professor with SIBET, Chinese Academy of Sciences (CAS).



NINGHAO WANG received the B.S. degree in mechanical engineering from Soochow University, Suzhou, China, in 2018. He is currently pursuing the master's degree with the University of Science and Technology of China. He is currently working at the Suzhou Institute of Biomedical Engineering and Technology, Chinese Academy of Sciences, under the supervision of Dr. Xiaohua Jian. His research interest includes high-frequency ultrasound imaging.



XIAOHUA JIAN (Member, IEEE) received the B.S. degree in optics information science and technology and the Ph.D. degree in physics from Xi'an Jiaotong University, China, in 2005 and 2011, respectively. In 2011, he joined the Suzhou Institute of Biomedical Engineering and Technology, Chinese Academy of Sciences, where he was promoted to Researcher, in 2017. His research interests include ultrasonic transducer design and fabrication, high frequency ultrasound system development, photoacoustic imaging, and optics spectroscopy.

...